A record of deep-ocean dissolved O_2 from the oxidation state of iron in submarine basalts

Daniel A. Stolper[1] & C. Brenhin Keller[1,2]

[1]Department of Earth and Planetary Science, University of California, Berkeley, California 94720, USA. [2]Berkeley Geochronology Center, Berkeley, California 94720, USA.

Abstract

The oxygenation of the deep ocean in the geological past has been associated with a rise in the partial pressure of atmospheric molecular oxygen (O_2) to near-present levels and the emergence of modern marine biogeochemical cycles[1,2,3,4,5]. It has also been linked to the origination and diversification of early animals[3,5,6,7]. It is generally thought that the deep ocean was largely anoxic from about 2,500 to 800 million years ago[1,2,3,4,5,6,7,8,9,10,11,12], with estimates of the occurrence of deep-ocean oxygenation and the linked increase in the partial pressure of atmospheric oxygen to levels sufficient for this oxygenation ranging from about 800 to 400 million years ago[3,5,7,11,13]. Deep-ocean dissolved oxygen concentrations over this interval are typically estimated using geochemical signatures preserved in ancient continental shelf or slope sediments, which only indirectly reflect the geochemical state of the deep ocean. Here we present a record that more directly reflects deep-ocean oxygen concentrations, based on the ratio of Fe^{3+} to total Fe in hydrothermally altered basalts formed in ocean basins. Our data allow for quantitative estimates of deep-ocean dissolved oxygen concentrations from 3.5 billion years ago to 14 million years ago and suggest that deep-ocean oxygenation occurred in the Phanerozoic (541 million years ago to the present) and potentially not until the late Palaeozoic (less than 420 million years ago).

Main

There is general agreement that between about 2,500 and 2,300 million years (Myr) ago, the partial pressure of oxygen in the atmosphere, $p_{O_2,atm}$, rose from below to above approximately 10^{-5} times present atmospheric levels (PAL)[1,2,4], and since about 400 Myr ago, $p_{O_2,atm}$ has remained above about 70% PAL[10,14,15]. Biogeochemical models suggest that $p_{O_2,atm}$ levels exceeding 15% (ref. 3) to 50% (ref. 1) PAL are needed to oxygenate the deep ocean. From about 2,500–800 Myr ago, it is generally thought[1,2,3,4,5,6,7,8,9,10,11,12] that $p_{O_2,atm}$ was below this threshold and that the deep ocean was either anoxic or contained at most a few micromoles of O_2 molecules per kilogram of seawater (μmol kg^{-1}) (modern deep-ocean O_2 concentrations average about 180 μmol kg^{-1})[16]. Estimates of when $p_{O_2,atm}$ exceeded these levels and the deep ocean became oxygenated range from 815 to 400 Myr ago[3,5,7,11,13]. Constraining the timing of deep-ocean oxygenation is important because it signals the beginning of

modern marine biogeochemical cycles and has been causally linked (owing to the implied rise in) to the Neoproterozoic origination of animals (which require O_2)[3,5,6,7,9,10].

Most reconstructions of Mesozoic and older deep-ocean geochemical conditions are based on the chemical and isotopic composition of continental shelf and slope sediments[3,4,5,9,10,11] deposited below the storm wave base[9] (deeper than about 100 m). Neoproterozoic to Early Phanerozoic sedimentary successions suggest that continental deep waters varied from oxic, to ferruginous, to sulfidic, depending on the formation studied[3,5,9,10,11], and record the geochemistry of spatially and temporally variable local water masses[9,10] instead of the deep, open ocean. Here we present a new proxy for past deep-ocean O_2concentrations based on $Fe^{3+}/\Sigma Fe$ ratios in ancient hydrothermally altered seafloor basalts.

Today, basalts erupt on the seafloor primarily as pillows and massive flows and are oxidized by oxygenated seawater circulating through oceanic crust. Basalts recovered during deep-sea drilling show that this circulation increases $Fe^{3+}/\Sigma Fe$ ratios from about 0.15 to 0.45 (±0.15)[17]. Although some of this iron may be oxidized via seawater hydrolysis[17], more than half[17] of all iron oxidation is mediated by O_2. We propose that $Fe^{3+}/\Sigma Fe$ ratios of hydrothermally altered oceanic basalts will be lower in anoxic versus oxygenated deep oceans and could therefore record changes in deep-ocean O_2 concentrations. Although most Mesozoic and older oceanic basalts have been lost via subduction, some are preserved on continents in ophiolite sequences[18]. Following ref. 18, we accept previously identified igneous oceanic crust preserved on continental crust as ophiolites. Finally, ref. 16 defines the modern deep ocean as deeper than 1,200 m—such waters have typical O_2 concentrations[16] of about 180 ± 80 μmol kg^{-1}, are deeper than most oxygen minimum zones[16], and span typical modern oceanic ridge depths (>2,500 m deep[19]).

We compiled $Fe^{3+}/\Sigma Fe$ ratios of ophiolitic basalts from the period 3,503–14 Myr ago (73 ophiolites and 1,085 $Fe^{3+}/\Sigma Fe$ determinations; Supplementary Table 1). Only data from extrusive, subaqueous basalts were compiled because these form the main conduit for seawater circulation through oceanic crust[17]. We additionally compiled $Fe^{3+}/\Sigma Fe$ ratios of Mesozoic–Cenozoic basalts recovered during deep-sea drilling (71 cores and 1,151 $Fe^{3+}/\Sigma Fe$ determinations; Supplementary Table 2).

Figure 1 shows average basalt $Fe^{3+}/\Sigma Fe$ ratios of each ophiolite versus age. We place the following bounds on $Fe^{3+}/\Sigma Fe$ ratios of unaltered oceanic basalts. Oceanic crust in ophiolites derives from a variety of settings including mid-ocean ridges and back-arc basins[18]. We take a lower $Fe^{3+}/\Sigma Fe$ bound for mid-ocean-ridge basalts (whole-rock) of 0.10 (ref. 17) and an upper bound of 0.31 based on Lau Basin back-arc glasses[20]. Mean Archaean (>2,500 Myr ago), Palaeo–Mesoproterozoic (2,500–1,000 Myr ago), and Neoproterozoic (1,000–541 Myr ago) $Fe^{3+}/\Sigma Fe$ ratios are $0.20 \pm$

0.04 (2 standard errors of the mean; s.e.m.), 0.26 ± 0.02 (2 s.e.m.), and 0.26 ± 0.05 (2 s.e.m.), respectively, and are within the range given for unaltered oceanic crust (0.10–0.31). Statistical pairwise testing (Methods; Extended Data Tables 1 and 2) shows that these means are statistically indistinguishable ($P > 0.05$).

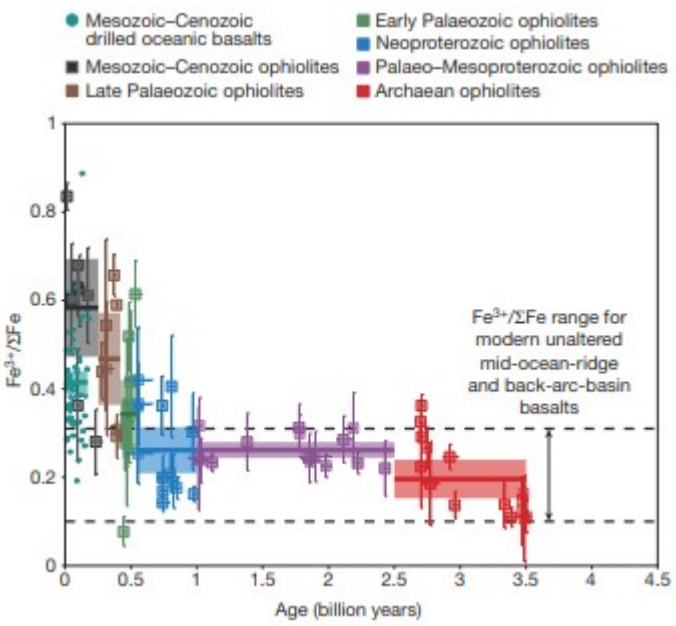

Figure 1: Average $Fe^{3+}/\Sigma Fe$ ratios of basalts from specific ophiolites and drilled oceanic crust.

Solid horizontal lines are sample averages over the given time period. Shading represents 2 s.e.m. uncertainty. $Fe^{3+}/\Sigma Fe$ error bars are 2 s.e.m. Age errors vary depending on the constraints available for each ophiolite (see Supplementary Table 1). Errors for drilled oceanic crust are not given for visual clarity, but are similar to those of the ophiolites. Dotted horizontal lines are the range of $Fe^{3+}/\Sigma Fe$ for modern mid-ocean-ridge and back-arc-basin basalts (see text). Ophiolite basalt $Fe^{3+}/\Sigma Fe$ ratios begin increasing in the Phanerozoic, indicating that the oxygenation of the deep ocean occurred in the Phanerozoic.

Phanerozoic ophiolite samples (<541 Myr old) have elevated $Fe^{3+}/\Sigma Fe$ ratios relative to Precambrian (>541 Myr old) and unaltered modern basalts and these ratios increase with time. Specifically, $Fe^{3+}/\Sigma Fe$ ratios of Early Palaeozoic ophiolite basalts (541–420 Myr old) average 0.34 ± 0.08 (2 s.e.m.); Late Palaeozoic basalts (420–252 Myr old) average 0.47 ± 0.10 (2 s.e.m.); and Mesozoic–Cenozoic basalts (< 252 Myr old) average 0.58 ± 0.11 (2 s.e.m.). We separate the Early and Late Palaeozoic because some studies argue for a Late Palaeozoic (approximately 420–400 Myr ago[7,10]) oxygenation of the deep ocean. Pairwise testing indicates that Mesozoic–Cenozoic and Late Palaeozoic versus Precambrian means are statistically different ($P < 0.05$). The Early Palaeozoic mean is statistically indistinguishable from the Late Palaeozoic and Neoproterozoic means ($P > 0.05$) but differs from the Mesozoic–Cenozoic, Palaeo–Mesoproterozoic, and Archaean means ($P < 0.05$), supporting the inference of a Phanerozoic increase in ophiolite $Fe^{3+}/\Sigma Fe$ ratios. $Fe^{3+}/\Sigma Fe$ ratios of Mesozoic–Cenozoic

drilled oceanic crust average 0.41 ± 0.03 (2 s.e.m.), which we discuss below.

Differences in $Fe^{3+}/\Sigma Fe$ ratios between Precambrian and Phanerozoic ophiolite basalts are apparent in data histograms (Fig. 2). Distributions for Precambrian ophiolites all show peak $Fe^{3+}/\Sigma Fe$ ratios of 0.1–0.3, with a tail to higher values (Fig. 2a–c); we suggest that this tail reflects the recent oxidation of a few samples at Earth's surface. A shift to higher $Fe^{3+}/\Sigma Fe$ ratios emerges in Early Palaeozoic ophiolites (Fig. 2d), as the peak $Fe^{3+}/\Sigma Fe$ ratio rises to 0.3–0.4. This increase continues through the Late Palaeozoic (peak from 0.5–0.7; Fig. 2e) to the Mesozoic–Cenozoic (peak from 0.6–0.8; Fig. 2f).

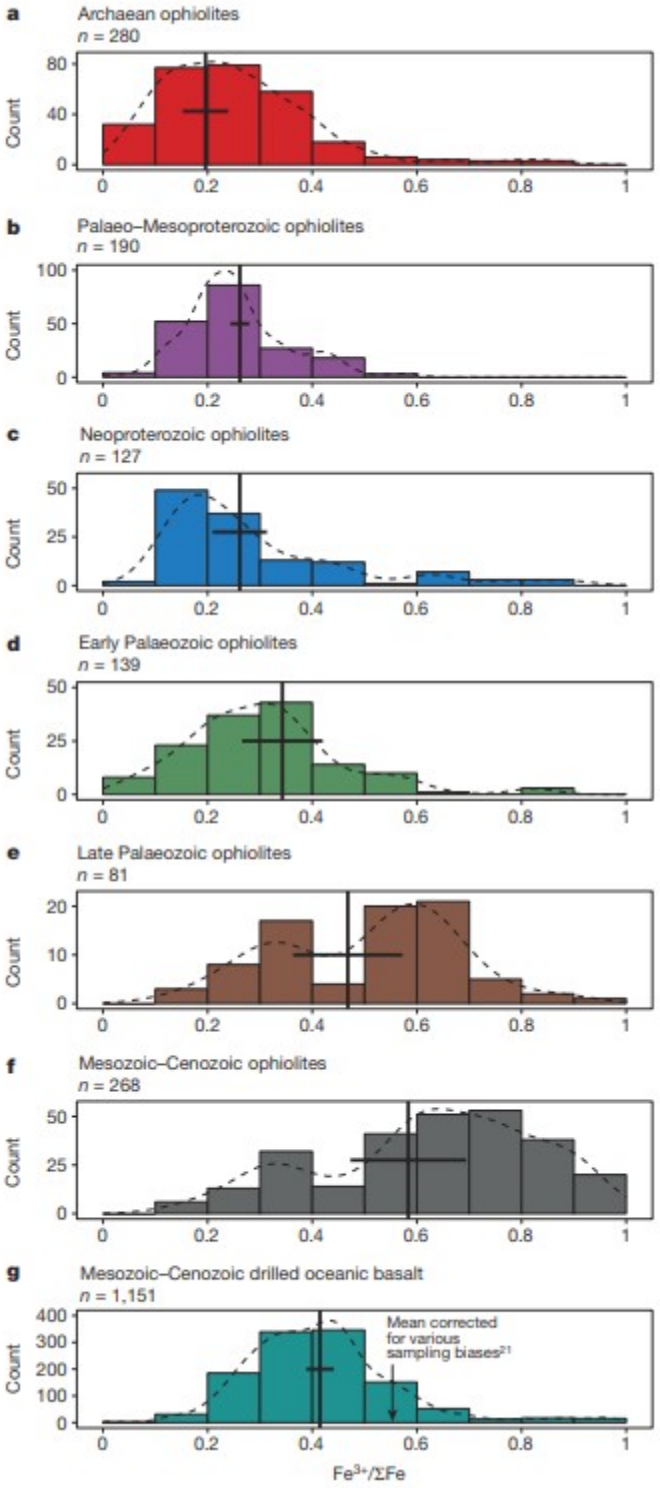

Figure 2: Histograms of $Fe^{3+}/\Sigma Fe$ ratios from individual samples as a function of time period.

a–g, Time periods are the same as those given in Fig. 1. The *y*-axis label 'Count' refers to the number of samples in a given $Fe^{3+}/\Sigma Fe$ bin. Solid black vertical lines are the mean values for a specific time period as given in Fig. 1, with horizontal 2 s.e.m. error bars. *n* is the number of data points. Dotted lines are smoothed distributions

(Methods). The difference between Phanerozoic and Precambrian $Fe^{3+}/\Sigma Fe$ ratios is clear both in the average value and in the distributions. g, The corrected mean for drilled oceanic crust is taken from ref. 21.

Late Palaeozoic and Mesozoic–Cenozoic ophiolites have bimodal $Fe^{3+}/\Sigma Fe$ distributions, with a minimum in the range 0.4–0.5. In contrast, the $Fe^{3+}/\Sigma Fe$ distribution of drilled Mesozoic–Cenozoic deep-sea basalts is unimodal, with a maximum (and mean) at about 0.4 (Fig. 2g). We suggest that differences in $Fe^{3+}/\Sigma Fe$ distributions and means between Mesozoic–Cenozoic ophiolites versus drilled oceanic basalts reflect an underestimation of average $Fe^{3+}/\Sigma Fe$ ratios in drilled samples. Specifically, averages of geochemical parameters from drilled oceanic crust can be biased by incomplete core recovery and preferential sampling of pristine or altered samples[17]. Data from Ocean Drilling Program sites 417 and 418 have been used to correct for these biases previously[21]. Mean $Fe^{3+}/\Sigma Fe$ ratios based on averaging all basalt data[17]at these sites range from 0.4–0.45, similar to our drill-core mean of 0.41 (±0.03, 2 s.e.m.). When this mean is calculated using both $Fe^{3+}/\Sigma Fe$ ratios and the relative abundance of various lithologies, this ‘weighted’ mean increases[21] to 0.56, indistinguishable from the Cenozoic–Mesozoic ophiolite mean (0.58 ± 0.011, 2 s.e.m.). Thus, we argue that mean $Fe^{3+}/\Sigma Fe$ ratios of cored and ophiolite Mesozoic–Cenozoic basalts are in agreement.

The observed Phanerozoic increase in $Fe^{3+}/\Sigma Fe$ ratios could result from several processes including temporal changes in basalt geochemical properties, in metamorphism, or in deep-ocean O_2 concentrations. If basalt iron contents were higher in the past, similar degrees of oxidation could result in smaller changes in $Fe^{3+}/\Sigma Fe$ ratios for older samples. On the basis of $Fe^{3+}/\Sigma Fe$ versus total iron and total iron versus age relationships (Extended Data Fig. 1), we calculate that this process could account for a change in $Fe^{3+}/\Sigma Fe$ ratios of 0.04 ± 0.03 (2σ) over the past 3.5 billion years in our data. A shift in ophiolite formational environments from mid-ocean ridges to back-arc basins could likewise increase initial basalt $Fe^{3+}/\Sigma Fe$ ratios[22]. However, basalt $Fe^{3+}/\Sigma Fe$ ratios from these environments typically differ[22] by <0.06. Consequently, these processes appear to be unlikely drivers for the >0.3 increase in $Fe^{3+}/\Sigma Fe$ ratios from the Neoproterozoic to Phanerozoic.

Alternatively, lower mean $Fe^{3+}/\Sigma Fe$ ratios of Precambrian versus Phanerozoic samples could reflect preferential metamorphic reduction of Fe^{3+} to Fe^{2+} in Precambrian samples. We consider the late oxidative alteration of samples (for example, occurring on the surface today) to be an unlikely cause of the $Fe^{3+}/\Sigma Fe$ record because this should affect all samples equally and thus does not explain the observed higher $Fe^{3+}/\Sigma Fe$ ratios for Phanerozoic versus Precambrian basalts. For metamorphic reduction to explain the record, it is necessary that $Fe^{3+}/\Sigma Fe$ ratios of Precambrian oceanic basalts first be elevated by oxidation above eruptive values (0.10–0.31) before metamorphic reduction returned them back to

their eruptive values, and that this did not occur in Phanerozoic samples. This is possible, because Precambrian ophiolites, owing to their age, are more likely to have experienced metamorphism than Phanerozoic equivalents. We note, however, that samples were selected from systems that retain primary igneous textures (for example, pillows), thus removing highly metamorphosed formations from consideration. Nonetheless, we designed two tests for a metamorphic influence on the $Fe^{3+}/\Sigma Fe$ record:

(1) We examined the relationship between $Fe^{3+}/\Sigma Fe$ and total iron for Precambrian ophiolite basalts (Extended Data Fig. 2); we expect that samples with lower total iron will be more susceptible to metamorphic reduction owing to the lower extent of reaction (that is, the total moles of Fe reduced) needed to reach chemical equilibrium. For these samples, the slope between total iron and $Fe^{3+}/\Sigma Fe$ is -0.003 (± 0.006, 2σ), which is indistinguishable from zero at the 2σ level, and thus is inconsistent with a metamorphic control on the $Fe^{3+}/\Sigma Fe$ record.

(2) We compiled $Fe^{3+}/\Sigma Fe$ ratios from continental volcanic rocks[23] from the past 3,850 Myr (8,335 individual measurements; Fig. 3 and Methods). This compilation includes subaerially erupted rocks, which we expect, following the oxygenation of the atmosphere 2,500–2,300 Myr ago, to be oxidized at the surface by O_2 shortly after eruption. If these rocks also show low $Fe^{3+}/\Sigma Fe$ until the Phanerozoic, it would support the general occurrence of metamorphic iron reduction in Precambrian rocks. This is not the case: from 3,850 Myr ago to 2,000 Myr ago, $Fe^{3+}/\Sigma Fe$ ratios of continental volcanics show mean values similar to those of ophiolite basalts (0.2–0.3), increase from 2,000 Myr ago to 1,500 Myr ago, and then remain approximately constant to the present (Fig. 3). We are unaware of common tectonic processes likely to produce such a specific global and temporal pattern of metamorphism in which continental volcanics preferentially escape reductive metamorphism in the Proterozoic while ophiolites do not. Rather, direct oxidation by atmospheric O_2 following the Proterozoic rise in (Fig. 3) provides a simple explanation for the increase in $Fe^{3+}/\Sigma Fe$ of continental volcanics from 2,000 to 1,500 Myr ago.

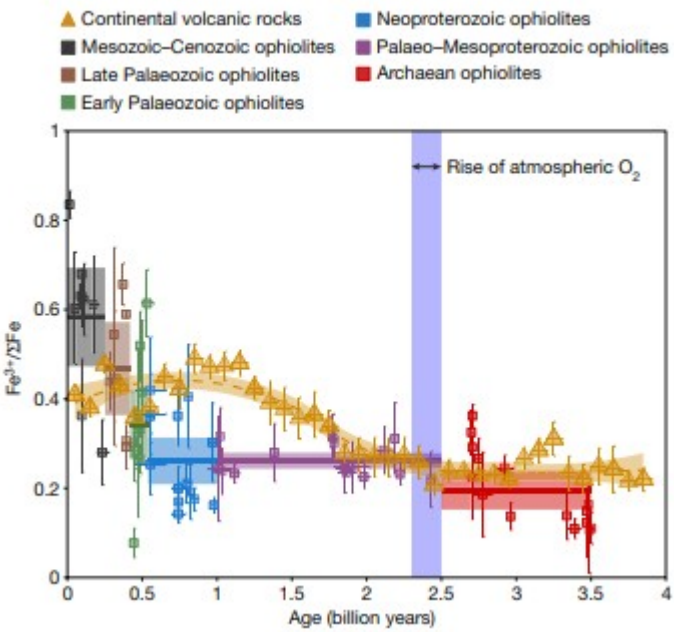

Figure 3: Comparison of $Fe^{3+}/\Sigma Fe$ ratios from ophiolite basalts versus continental volcanic rocks (including subaerial volcanics).

Ophiolite data are the same as in Fig. 1. Continental volcanic $Fe^{3+}/\Sigma Fe$ ratios are means of 100-million-year age bins with 2 s.e.m. error bars[23]. The dotted orange line is a smoothed moving average through the continental volcanic data with a shaded 95% confidence interval (Methods). Continental volcanics increase in $Fe^{3+}/\Sigma Fe$ from 2 to 1.5 billion years ago, more than a billion years before the rise in the ophiolite basalts. This indicates that reductive metamorphism is an unlikely cause of the difference in $Fe^{3+}/\Sigma Fe$ between Phanerozoic and Precambrian ophiolite basalts.

Consequently, we propose that the Phanerozoic increase in $Fe^{3+}/\Sigma Fe$ ratios of ophiolitic basalts reflects an increase in the hydrothermal flux of O_2 into oceanic crust. One possibility is that a large increase in the flux of already oxygenated seawater through oceanic crust occurred in the Phanerozoic. However, higher fluxes of seawater through oceanic crust have been proposed for the Precambrian relative to the Phanerozoic[24] and hydrothermally altered basalts as old[25] as 3,500 Myr can be found. We therefore consider a large Phanerozoic increase in the flux of seawater through oceanic crust an unlikely driver of the $Fe^{3+}/\Sigma Fe$ record.

Instead, we propose that the Phanerozoic increase in $Fe^{3+}/\Sigma Fe$ ratios of submarine basalts marks the oxygenation of the deep ocean. We now use this record to estimate past deep-ocean O_2 concentrations, employing a model (Methods) that balances the O_2 flux needed to increase basaltic $Fe^{3+}/\Sigma Fe$ ratios from initial (0.10–0.31) to measured values against the minimum seawater O_2 concentration required to supply this flux during hydrothermal alteration of oceanic crust. Modelled O_2 concentrations are minimum estimates because we assume complete reduction of O_2 entering oceanic crust.

Calculated deep-ocean O_2 concentrations are given in Fig. 4a and compared to independent estimates of $p_{O_2,atm}$ in Fig. 4b. Calculated average Archaean deep-ocean O_2 concentrations are -3 ± 18 μmol kg^{-1} (2 s.e.m.) and are consistent with the general expectation of an anoxic Archaean deep ocean[2,4,11,12]. Mean calculated Palaeo–Mesoproterozoic and Neoproterozoic O_2 concentrations are 11 ± 17 μmol kg^{-1} (2 s.e.m.) and 11 ± 20 μmol kg^{-1} (2 s.e.m.). Both are within 2 s.e.m. of the anoxic level, broadly compatible with the common view of an anoxic Proterozoic deep ocean[1,2,4,5,6,11,12], while also allowing for suggestions[8]of low (of the order of micromoles per kilogram of seawater) Proterozoic deep-ocean O_2 concentrations. Calculated average Early to Late Palaeozoic deep-ocean O_2 concentrations are 29 ± 29 μmol kg^{-1} (2 s.e.m.) and 55 ± 42 μmol kg^{-1} (2 s.e.m.). These concentrations compare favourably to estimated minimum O_2 concentrations required for Phanerozoic fauna[7] (more than 15–30 μmol kg^{-1}). Calculated Mesozoic–Cenozoic deep-ocean O_2 concentrations are 80 ± 53 μmol kg^{-1} (2 s.e.m.), about 45% of modern average deep-ocean O_2 concentrations (178 μmol kg^{-1})[16]. This difference could result if only about 45% of all O_2 that enters oceanic crust is reduced, as opposed to the assumed 100%, which is acceptable given that our calculations are minimum estimates. Alternatively, some estimates of Mesozoic are as low as 60%–70% of modern[26], which would support our estimated lower-than-modern Mesozoic deep-ocean O_2 concentrations.

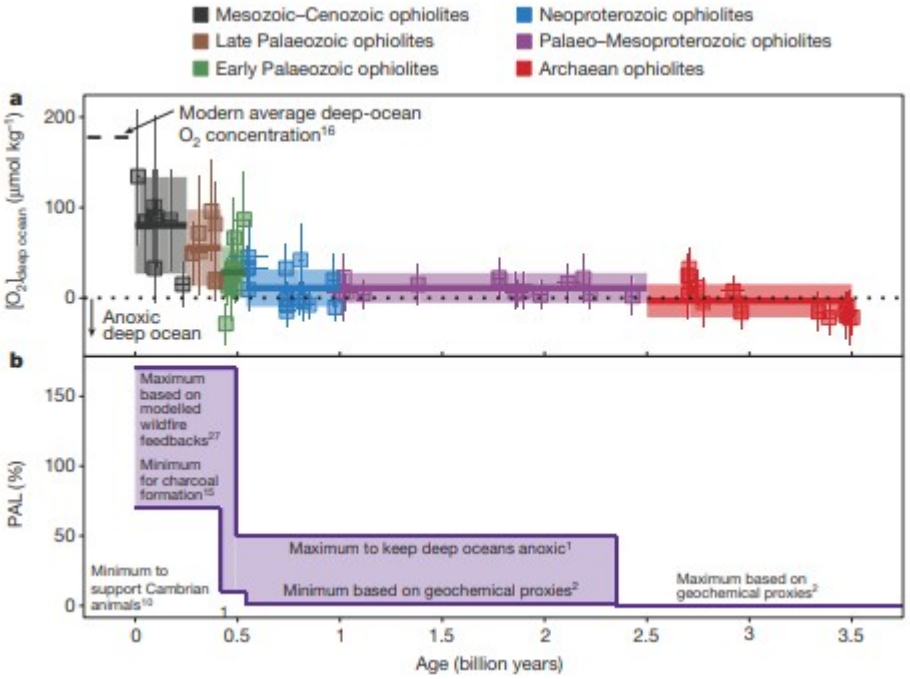

Figure 4: Calculated deep-ocean O_2 concentrations versus time compared to previous estimates of $p_{O_2,atm}$.

a, Calculated deep-ocean O_2 concentrations (in micromoles O_2 per kilogram of seawater) based on $Fe^{3+}/\Sigma Fe$ ratios of ophiolite basalts (Methods). Bold horizontal lines are averages for a given time period, with shading representing 2 s.e.m.

O_2 concentration error bars are 2 s.e.m. b, Ranges of estimated allowable atmospheric O_2 levels are given as present atmospheric levels (PAL), that is, as a percentage of modern levels, and are based on refs 1, 2, 10, 15 and 27. b is in part modelled after a figure in ref. 10.

We propose that ophiolite $Fe^{3+}/\Sigma Fe$ ratios provide direct, quantitative constraints on the O_2 content of the deep ocean from the Archaean to the Cenozoic. In particular, they indicate that the deep ocean became oxygenated only in the Phanerozoic and probably not until the late Palaeozoic (<420 Myr; Fig. 4a). This is consistent with some previous studies[7,10,27] (Fig. 4b) but contrasts with proposals for a Precambrian oxygenation of the deep ocean[5,11]. This result is important because it provides direct evidence that the rise in $p_{O_2,atm}$ to levels sufficient to oxygenate the deep ocean (PAL >15%–50%)[1,3] postdates by hundreds of millions of years the Neoproterozoic origination of animals and is thus causally unrelated to this event.

What caused the rise in $p_{O_2,atm}$ that oxygenated the deep ocean and why it postdates the oxygenation of the atmosphere by about 2 billion years is debated, with hypotheses ranging from the radiation of vascular plants[27] to perturbations in global biogeochemical cycles due to Neoproterozoic glaciations[3,5,28]. These hypotheses generally predict rapid (<50 Myr) increases in $p_{O_2,atm}$ to levels sufficient to oxygenate the deep ocean. Additionally, models typically find that Late Palaeozoic $p_{O_2,atm}$ was higher[26] or similar[27] to Mesozoic and Cenozoic . In contrast, the ophiolite $Fe^{3+}/\Sigma Fe$ record suggests that deep-ocean O_2concentrations and thus $p_{O_2,atm}$ (assuming the two correlate) increased steadily over the entire Phanerozoic. This would indicate that $p_{O_2,atm}$ is regulated by feedbacks that strongly minimize imbalances in O_2 sources and sinks on million-year timescales, preventing large oscillations in . Such a minimization of these imbalances appears to have occurred over the past million years[29].

Finally, the oxygenation of the deep ocean also probably affected the solid Earth. This oxygenation would have led to increased $Fe^{3+}/\Sigma Fe$ ratios in oceanic crust and more oxidized sediments in subducting slabs. This in turn would have increased the subducted flux of oxidized materials to the mantle over the past 540 Myr and caused a progressive oxidation of the mantle over the Phanerozoic. This hypothesis provides a straightforward explanation for invariant estimated upper-mantle oxygen fugacities of modern versus Archaean basalts[30], despite proposals for an increase in mantle oxygen fugacity two to three billion years ago[31] owing to subduction of oxidized Archaean slabs—simply put, such slabs did not become substantially oxidized until the Phanerozoic oxygenation of the deep ocean. This hypothesis is consistent with proposed changes in the uranium isotopic composition of altered oceanic crust and the mantle with time[32] and is testable as follows. If correct, $Fe^{3+}/\Sigma Fe$ ratios should be higher in Phanerozoic than in Precambrian island-arc rocks if arc magmas are

oxidized (as some believe[22]) owing to interactions with oxidized fluids derived from oxidized slabs.

Methods

Data compilation

Ophiolite basalt $Fe^{3+}/\Sigma Fe$ ratios were compiled from primary studies with reported FeO and Fe_2O_3 values. Data are derived from samples described in previous studies either as subaqueous basalts from ophiolites or preserved oceanic crust. Samples were often identified using previous compilations of Phanerozoic and Precambrian ophiolites[18,33,34,35]. Studies where Fe_2O_3 values were calculated based on measurements of total FeO contents and assumed FeO/Fe_2O_3 or Fe^{3+}/Fe^{2+} ratios were not used because the Fe_2O_3 values were not independently measured. Additionally, data from Jurassic–Triassic-aged ophiolites in the Brooks Range, Alaska, described in ref. 36, were not used. This study was not used because data were corrected for post-formational oxidative alteration by assuming a relationship between TiO_2 and Fe_2O_3 content. Samples with excess Fe_2O_3 relative to this relationship were assumed to have been altered (though whether this alteration occurred during seafloor alteration or later is not stated) and the excess Fe_2O_3 was converted back to FeO in an attempt to restore the samples to their original igneous compositions. Problematically, which samples were corrected and the originally measured, uncorrected Fe_2O_3 values are not given. As we are interested in a sample's Fe_2O_3 value due to hydrothermal alteration, this study could not be used.

All ophiolite data are given in Supplementary Table 1. We additionally provide in Supplementary Table 1 other major element data, sample descriptions, and age constraints.

For oceanic-basalt data from deep-sea drill cores, $Fe^{3+}/\Sigma Fe$ ratios were compiled from cores taken by the Deep-Sea Drilling Program and its later iterations. Only data for samples older than 10 Myr were used because such samples are thought to have seen sufficient integrated fluid fluxes to reach near-maximum $Fe^{3+}/\Sigma Fe$ ratios[17,37]. Data were derived from original deep-sea drilling reports, as given in Supplementary Table 2. Average values for cores are presented in Fig. 1and were derived by weighting $Fe^{3+}/\Sigma Fe$ versus depth relative to the depth span defined by the data. This was done to prevent a large number of samples measured from a specific horizon (for example from a vein) from carrying undue weight in the final average. Doing this generally resulted in minimal differences (<0.05) in final $Fe^{3+}/\Sigma Fe$ ratios versus averaging all of the data.

Continental volcanic data were compiled using a database of geochemical measurements[23]. We also included in this database $Fe^{3+}/\Sigma Fe$ ratios from approximately 2-billion-year-old subaerial volcanic rocks recovered from drilling in Fennoscandia[38]. Only igneous rocks with SiO_2 compositions of 40–

80 wt% were included in the original[23]compilation (which carries forward to our use of the database). Data were resampled and standard errors of the means for age bins of 100 Myr were calculated following the methodology described in ref. 23. To ensure that the database did not include publications in which $Fe^{3+}/\Sigma Fe$ or FeO/Fe_2O_3 values were assumed or assigned a constant value (in order to calculate an Fe_2O_3 weight per cent value based on an FeO weight per cent measurement for example or vice versa), we removed data from consideration from any publication in which the relative $FeO/(Fe_2O_3+FeO)$ standard deviation (standard deviation/mean) was less than 1%. This removes about 14% of all data, but does not change any trends noticeably.

This continental volcanic data set contains both subaerial and subaqueous volcanic rocks preserved on continental crust. 96% of rocks in the record younger than 100,000 years old are currently found above sea level (and thus probably formed subaerially). How the proportion of subaerial versus subaqueous volcanism changes over time in this database is unknown. However, it has been argued on the basis of abundances of preserved subaqueous versus subaerial large igneous provinces that a large increase in proportion of subaerial versus subaqueous volcanism occurred 2.5 billion years ago[39] (an increase from about 20% to 70%) with relatively stable proportions of subaerial versus subaqueous large igneous province formation from that point onwards. If proportions of subaerial versus subaqueous volcanism for samples from our database mirror the large-igneous-province record, then more than 60% of continental volcanics have formed subaerially since 2.5 billion years ago. If this is correct, then we consider it unlikely that the increase in continental volcanic $Fe^{3+}/\Sigma Fe$ ratio values observed 2 billion years ago (Fig. 3) is linked to changes in proportions of subaerial versus subaqueous volcanism.

Data smoothing

In Fig. 2, a smoothed data distribution (given by the black dotted lines) is presented along with discrete histograms. This smoothed histogram was calculated using the default parameters of the stat_smooth function in the R statistical software package[40]. In Fig. 3, a moving average for the continental volcanic data was given with 95% confidence intervals. It was made using the geom_smooth function with a span of 0.75 in the R statistical software package[40].

Statistical testing

Whether mean $Fe^{3+}/\Sigma Fe$ ratios of various age bins are statistically distinct or not was tested using pairwise testing with a *P*-value cut-off of 0.05, with <0.05 indicating that averages are distinct and >0.05 indicating they are indistinguishable. Two tests were used, the parametric Tukey–HSD test and the non-parametric Wilcoxon test. For the Wilcoxon test, we used the Holm *P*-adjustment method. All tests were performed using functions

encoded in the R statistical software package[40]. The *P* values for all pairwise tests are given below in Extended Data Tables 1 and 2.

Modelling dissolved O_2 concentrations

O_2 concentrations were calculated based on measured $Fe^{3+}/\Sigma Fe$ ratios using a mass-balance-based model. This model assumes that a certain volume of crust is produced each year that will have potentially oxidizing seawater flow through it (generally restricted to the top 500 ± 200 m of igneous oceanic crust[17]). It then assumes a certain average weight per cent of iron in the rock produced and uses a specific ophiolite's or average time period's $Fe^{3+}/\Sigma Fe$ ratio value relative to an assumed initial value to calculate the amount of iron oxidized per year in oceanic crust. We assume that the initial $Fe^{3+}/\Sigma Fe$ ratios range from 0.1 to 0.31 (with a uniform distribution); this is the range discussed in the main text for unaltered modern oceanic basalts.

We additionally account for the oxidation of igneous sulphur in oceanic crust. Our compilation lacks measurements of sulphur either in amount or redox state. We assume that all sulphur in the erupted igneous rocks is present as sulphide based on sulphide saturation in mid-ocean-ridge basalts[41]. To calculate the amount of sulphur oxidized in the samples, we assume (for lack of any other constraints) that the ratio of sulphur versus iron oxidation (in moles) observed in modern mid-ocean-ridge basalts has remained constant through time. Thus, from the shift in $Fe^{3+}/\Sigma Fe$ measured in our samples, we can calculate the amount of sulphur that would have been oxidized as well.

We balance the O_2 demand indicated by moles of iron and sulphur oxidized in oceanic crust by an input flux of O_2 into oceanic crust from the deep ocean. This is calculated by multiplying the concentration of O_2 in the deep ocean by the flux of seawater into oceanic crust. As discussed in the main text, in doing this, we assume that all O_2 that is delivered into oceanic crust is consumed via the oxidation of reduced minerals, making our calculations of deep-ocean O_2 concentrations a minimum estimate because some fluids may emerge from oceanic crust with O_2 remaining. Since altered oceanic crust contains secondary minerals that formed in both oxic and anoxic environments[42], it follows that fluids can lose all of their oxygen during circulation. We are unaware of any studies measuring the oxygen concentration of waters flowing out of oceanic crust into the ocean at temperatures <100 °C (hot hydrothermal fluids are anoxic), which would offer a means of testing this assumption.

An additional assumption made is that fluids flowing through oceanic crust today and in the past are sourced from waters that are representative of average deep-ocean water masses. Deep-ocean O_2concentrations vary as a function of the integrated amount of respiration that has occurred in the deep ocean. Average modern deep-ocean waters (>1,200 m deep) have O_2 concentrations of about 180 μmol kg^{-1}, and typically are within ±80

μmol kg^{-1} of this number[16]. However, so-called 'oxygen minimum zones' exist in the ocean, where O_2concentrations can decline[16] to below 10 μmol kg^{-1}. Such water masses are typically restricted to depths[43] shallower than 1,000 m. In contrast, modern spreading centres have typical ocean depths[19] greater than 2,500 m, and thus occur at ocean depths deeper than those at which oxygen minimum zones occur. Instead, fluids flowing through modern oceanic crust are derived from water masses with O_2 concentrations similar to mean deep-ocean (>1,200 m depth) O_2 concentrations[16] (180 ± 80 μmol kg^{-1}). We note that the depths of oceans may have varied in the past, but the direction of change is unknown and debated[19]. Thus we make what we consider the simplest assumption: that waters flowing through past oceanic basalts track average deep-ocean O_2concentrations.

The full equation used to balance O_2 consumed versus O_2 supplied to oceanic crust is:

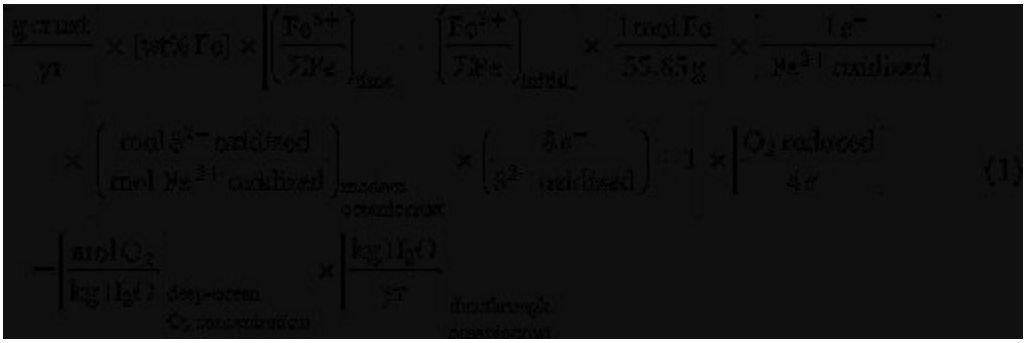

In equation (1), e^- is an electron.

To calculate deep-ocean O_2 concentrations, we solve equation (1) for '[mol O_2/kg H_2O]$_{\text{deep-ocean O2 concentration}}$', the first term on the right side of the equation. The term '$(Fe^{3+}/\Sigma Fe)_{time}$' is taken from our data. All other terms are either constants or are taken from the literature.

We take the amount of crust generated per year that sees potentially oxidizing fluids to be 4.0×10^{15} g yr^{-1} with a uniformly distributed error of $\pm 1.8 \times 10^{15}$ g yr^{-1} as given in ref. 17. In that study[17], the distribution and level of uncertainty reported is not given (for example, whether Gaussian, and, if so, whether the given uncertainty is 1σ or 2σ). Although a stated uncertainty often implies a Gaussian distribution, many quantities that cannot take negative values, such as crustal production rates, are fundamentally incompatible with a Gaussian distribution. To avoid this, we chose a uniform distribution for the error, and assumed that the reported uncertainties above represent the full range of values.

We assume an average weight per cent of Fe of $8\% \pm 0.7\%$ in oceanic basalts. This is derived from ref. 17, where the error is described as 1σ(and thus has a Gaussian distribution). This value is consistent with other

compilations of mid-ocean-ridge-basalt chemical data including that from ref. 44 (7.8% ± 2.9%, 2σ) and ref. 45 (8.1% ± 0.2%, 95% confidence interval).

$Fe^{3+}/\Sigma Fe$ ratios are taken from the ophiolite data. Errors are treated as normally distributed.

The number of moles of S^{2-} oxidized per year in modern oceanic crust is taken as $(1.1 \pm 0.7) \times 10^{11}$ mol yr^{-1}. The number of moles of Fe oxidized per year in modern oceanic crust is taken as $(1.7 \pm 1.2) \times 10^{12}$ mol yr^{-1}. Both values are from ref. 17 and the errors are treated as uniformly distributed for the same reasons as discussed above for crustal production.

We take the values for the flux of seawater to oceanic crust from ref. 46. This study provides modelled estimates of this flux for the past 200 Myr, with ranges from 9×10^{15} to 1.5×10^{16} kilograms of H_2O per year. This overlaps with the range predicted in other calculations[47]. We incorporate the range of estimates for fluid fluxes into our error propagation by randomly sampling a data point from the seawater flux versus time curve (0–200 Myr) in figure 3C of ref. 46. In our error propagation scheme, we take a random number from a uniform, integer distribution from 0 to 200, multiply that number by one million, and then use that number as an age to derive a random seawater flux value from the past 200 Myr.

With all of these various error estimates, we perform a Monte Carlo error propagation scheme to solve equation (1). Specifically, equation (1) is solved for '$[\text{mol } O_2/\text{kg } H_2O]_{\text{deep-ocean O2}}$ concentration' fifty million times for a given input $Fe^{3+}/\Sigma Fe$ ratio (and accompanying error) with numbers for all terms that are not constants drawn from the distributions discussed above.

The sensitivity of the model to calculated O_2 concentrations is straightforward because all terms in equation are multiplicative and do not (in our formulation) depend on each other. For example, a twofold increase in Fe weight per cent of basalts (which is on the left side of equation (1)), demands that O_2 concentrations also increase by twofold. Given that the errors on many terms are greater than ±50% relative, we consider our overall error based on the Monte Carlo simulation to be conservative.

We note that a question with this modelling approach is whether ophiolite $Fe^{3+}/\Sigma Fe$ ratios are representative of average oceanic basalt. As discussed in the main text, when mean $Fe^{3+}/\Sigma Fe$ ratios from the Mesozoic–Cenozoic are corrected for sampling biases and poor recovery, they agree with the ophiolite mean for the Mesozoic–Cenozoic (0.56 versus 0.58; see main text). Additionally, ophiolites have long been used to study the hydrothermal alteration of oceanic crust at both low (<100 °C) and high (>100 °C) temperatures in the past[48,49].

An alternative approach to the model is to normalize all ophiolite data to ophiolites. That is, if we assume, as is typically done, that the Archaean ocean was anoxic[2,4], we can normalize the starting data to the average

Archaean ophiolite basalt $Fe^{3+}/\Sigma Fe$ ratio of 0.20 ± 0.04 (2 s.e.m.). For comparison, we have taken the mean $Fe^{3+}/\Sigma Fe$ ratio for unaltered oceanic crust to be 0.205 (the midpoint of 0.10–0.31). As the two are similar (within 0.005 for $Fe^{3+}/\Sigma Fe$ ratios), normalizing to Archaean ophiolites has little effect on the model-derived deep-ocean O_2 concentrations, providing confidence in our approach.

Data availability

All $Fe^{3+}/\Sigma Fe$ ratios compiled for this work are available within the paper and its Supplementary Information.

References

1. Canfield, D. E. in *Treatise on Geochemistry* (eds Holland, H. D. & Turekian, K. K.) 197–216 (Elsevier, 2014)

2. Canfield, D. E. The early history of atmospheric oxygen: homage to Robert M. Garrels. *Annu. Rev. Earth Planet. Sci.* 33, 1–36 (2005)

3. Canfield, D. E., Poulton, S. W. & Narbonne, G. M. Late-Neoproterozoic deep-ocean oxygenation and the rise of animal life. *Science* 315, 92–95 (2007)

4. Lyons, T. W., Reinhard, C. T. & Planavsky, N. J. The rise of oxygen in Earth's early ocean and atmosphere. *Nature* 506, 307–315 (2014)

5. Sahoo, S. K. *et al.* Ocean oxygenation in the wake of the Marinoan glaciation. *Nature* 489, 546–549 (2012)

6. Planavsky, N. J. *et al.* Low Mid-Proterozoic atmospheric oxygen levels and the delayed rise of animals. *Science* 346, 635–638 (2014)

7. Dahl, T. W. *et al.* Devonian rise in atmospheric oxygen correlated to the radiations of terrestrial plants and large predatory fish. *Proc. Natl Acad. Sci. USA* 107, 17911–17915 (2010)

8. Slack, J., Grenne, T., Bekker, A., Rouxel, O. & Lindberg, P. Suboxic deep seawater in the late Paleoproterozoic: evidence from hematitic chert and iron formation related to seafloor-hydrothermal sulfide deposits, central Arizona, USA. *Earth Planet. Sci. Lett.* 255, 243–256 (2007)

9. Canfield, D. E. *et al.* Ferruginous conditions dominated later Neoproterozoic deep-water chemistry. *Science* 321, 949–952 (2008)

10. Sperling, E. A. *et al.* Statistical analysis of iron geochemical data suggests limited late Proterozoic oxygenation. *Nature* 523, 451–454 (2015)

11. Scott, C. *et al.* Tracing the stepwise oxygenation of the Proterozoic ocean. *Nature* 452, 456–459 (2008)

12. Canfield, D. E. A new model for Proterozoic ocean chemistry. *Nature* 396, 450–453 (1998)

13. Blamey, N. J. *et al.* Paradigm shift in determining Neoproterozoic atmospheric oxygen. *Geology* 44, 651–654 (2016)

14. Scott, A. C. & Glasspool, I. J. The diversification of Paleozoic fire systems and fluctuations in atmospheric oxygen concentration. *Proc. Natl Acad. Sci. USA* 103, 10861–10865 (2006)

15. Belcher, C. & McElwain, J. Limits for combustion in low O_2redefine paleoatmospheric predictions for the Mesozoic. *Science*321, 1197–1200 (2008)

16. Sarmiento, J. L. & Gruber, N. *Ocean Biogeochemical Dynamics*(Princeton Univ. Press, 2006)

17. Bach, W. & Edwards, K. J. Iron and sulfide oxidation within the basaltic ocean crust: implications for chemolithoautotrophic microbial biomass production. *Geochim. Cosmochim. Acta* 67, 3871–3887 (2003)

18. Dilek, Y. & Furnes, H. Ophiolite genesis and global tectonics: geochemical and tectonic fingerprinting of ancient oceanic lithosphere. *Geol. Soc. Am. Bull.* 123, 387–411 (2011)

19. Kasting, J. F. *et al.* Paleoclimates, ocean depth, and the oxygen isotopic composition of seawater. *Earth Planet. Sci. Lett.* 252, 82–93 (2006)

20. Nilsson, K. & Peach, C. L. Sulfur speciation, oxidation state, and sulfur concentration in backarc magmas. *Geochim. Cosmochim. Acta* 57, 3807–3813 (1993)

21. Staudigel, H., Plank, T., White, B. & Schmincke, H. U. Geochemical fluxes during seafloor alteration of the basaltic upper oceanic crust: DSDP Sites 417 and 418. *Geophys. Monogr. Ser.* 96, 19–38 (1996)

22. Kelley, K. A. & Cottrell, E. Water and the oxidation state of subduction zone magmas. *Science* 325, 605–607 (2009)

23. Keller, C. B. & Schoene, B. Statistical geochemistry reveals disruption in secular lithospheric evolution about 2.5 Gyr ago. *Nature* 485, 490–493 (2012)

24. Halevy, I. & Bachan, A. The geologic history of seawater pH. *Science* 355, 1069–1071 (2017)

25. Hofmann, A. & Harris, C. Silica alteration zones in the Barberton greenstone belt: a window into subseafloor processes 3.5–3.3 Ga ago. *Chem. Geol.* 257, 221–239 (2008)

26. Berner, R. A. Phanerozoic atmospheric oxygen: new results using the GEOCARBSULF model. *Am. J. Sci.* 309, 603–606 (2009)

27. Bergman, N. M., Lenton, T. M. & Watson, A. J. COPSE: a new model of biogeochemical cycling over Phanerozoic time. *Am. J. Sci.* 304, 397–437 (2004)

28. Laakso, T. A. & Schrag, D. P. Regulation of atmospheric oxygen during the Proterozoic. *Earth Planet. Sci. Lett.* 388, 81–91 (2014)

29. Stolper, D. A., Bender, M. L., Dreyfus, G. B., Yan, Y. & Higgins, J. A.Pleistocene ice core record of atmospheric O_2 concentrations. *Science* 353, 1427–1430 (2016)

30. Li, Z.-X. A. & Lee, C.-T. A. The constancy of upper mantle fO_2through time inferred from V/Sc ratios in basalts. *Earth Planet. Sci. Lett.* 228, 483–493 (2004)

31. Kump, L. R., Kasting, J. F. & Barley, M. E. Rise of atmospheric oxygen and the “upside-down” Archean mantle. *Geochem. Geophys. Geosyst.* 2, 1025 (2001)

32. Andersen, M. B. *et al.* The terrestrial uranium isotope cycle. *Nature* 517, 356–359 (2015)

33. Furnes, H., Dilek, Y. & De Wit, M. Precambrian greenstone sequences represent different ophiolite types. *Gondwana Res.* 27, 649–685 (2015)

34. Furnes, H., De Wit, M. & Dilek, Y. Four billion years of ophiolites reveal secular trends in oceanic crust formation. *Geosci. Front.* 5, 571–603 (2014)

35. Lécuyer, C. & Ricard, Y. Long-term fluxes and budget of ferric iron: implication for the redox states of the Earth’s mantle and atmosphere. *Earth Planet. Sci. Lett.* 165, 197–211 (1999)

36. Pallister, J. S., Budahn, J. R. & Murchey, B. L. Pillow basalts of the Angayucham terrane: oceanic plateau and island crust accreted to the Brooks Range. *J. Geophys. Res. Solid Earth* 94, 15901–15923 (1989)

37. Johnson, H. P. & Semyan, S. W. Age variation in the physical properties of oceanic basalts: implications for crustal formation and evolution. *J. Geophys. Res. Solid Earth* 99, 3123–3134 (1994)

38. Rybacki, K., Kump, L., Hanski, E. & Melezhik, V. Weathering during the Great Oxidation Event: Fennoscandia, arctic Russia 2.06 Ga ago. *Precambr. Res.* 275, 513–525 (2016)

39. Kump, L. R. & Barley, M. E. Increased subaerial volcanism and the rise of atmospheric oxygen 2.5 billion years ago. *Nature* 448, 1033–1036 (2007)

40. *R: A Language and Environment for Statistical Computing* (R Foundation for Statistical Computing, 2015); https://www.r-project.org

41. Wallace, P. & Carmichael, I. S. Sulfur in basaltic magmas. *Geochim. Cosmochim. Acta* 56, 1863–1874 (1992)

42. Alt, J. C. & Honnorez, J. Alteration of the upper oceanic crust, DSDP site 417: mineralogy and chemistry. *Contrib. Mineral. Petrol.*87, 149–169 (1984)

43. Karstensen, J., Stramma, L. & Visbeck, M. Oxygen minimum zones in the eastern tropical Atlantic and Pacific oceans. *Prog. Oceanogr.*77, 331–350 (2008)

44. Keller, C. B., Schoene, B., Barboni, M., Samperton, K. M. & Husson, J. M. Volcanic-plutonic parity and the differentiation of the continental crust. *Nature* 523, 301–307 (2015)

45. Gale, A., Dalton, C. A., Langmuir, C. H., Su, Y. & Schilling, J. G. The mean composition of ocean ridge basalts. *Geochem. Geophys. Geosyst.* 14, 489–518 (2013)

46. Müller, R., Dutkiewicz, A., Seton, M. & Gaina, C. Seawater chemistry driven by supercontinent assembly, breakup, and dispersal. *Geology* 41, 907–910 (2013)

47. Elderfield, H. & Schultz, A. Mid-ocean ridge hydrothermal fluxes and the chemical composition of the ocean. *Annu. Rev. Earth Planet. Sci.* 24, 191–224 (1996)

48. Gregory, R. T. & Taylor, H. P. An oxygen isotope profile in a section of Cretaceous oceanic crust, Samail Ophiolite, Oman: evidence for $\delta^{18}O$ buffering of the oceans by deep (> 5 km) seawater-hydrothermal circulation at mid-ocean ridges. *J. Geophys. Res. Solid Earth* 86, 2737–2755 (1981)

49. Bickle, M. J. & Teagle, D. A. Strontium alteration in the Troodos ophiolite: implications for fluid fluxes and geochemical transport in mid-ocean ridge hydrothermal systems. *Earth Planet. Sci. Lett.*113, 219–237 (1992)

Acknowledgements

D.A.S. acknowledges discussions with M. Bender, B. Buffett, D. DePaolo, J. Eiler, S. Finnegan, W. Fischer, J. Higgins, A. Saal and E. Stolper. We thank D. Canfield for advice on a prior draft. C.B.K. acknowledges support from the Ann and Gordon Getty Foundation.